ADVANCED MATERIALS

the present hollow silver spheres are much smaller than the previous hollow calcite spheres (ca. 3.4 μm), which could be attributed to the stronger coordination interaction of the anionic PMAA block with Ag^+ ions than with Ca^{2+} ions. This stronger coordination interaction could also be a large contributory factor to the considerable increase of the minimum SDS concentration required for the formation of hollow spheres, i.e., from 1 mM SDS for hollow calcite spheres to 10 mM SDS for hollow silver spheres. In other words, the presence of free PEO-*b*-PMAA molecules in the solution at a lower SDS concentration would be helpful for calcite precipitation around the complex micelles as the polymer acts as an inhibitor,[17] but would induce separate silver precipitation away from the complex micelles due to the formation of PEO-*b*-PMAA–Ag^+ complex.[28]

In conclusion, submicrometer-sized hollow silver spheres were successfully synthesized by using PEO-*b*-PMAA–SDS complex micelles as templates. The unique silver shell structures obtained here may be promising candidates for both fundamental research and applications. It is believed that templated synthesis based on polymer–surfactant complex micelles represents a novel route to inorganic hollow spheres, which is a topic of intense interest.

Experimental

A commercial DHBC, poly(ethylene oxide)-*block*-poly (methacrylic acid) (PEO-*b*-PMAA, PEO = 3000 g/mol, PMAA = 700 g/mol, T. Goldschmidt AG) [26], was used in this work. The anionic PMAA block carries carboxylate groups capable of coordinating with Ag^+ ions, whereas the non-ionic PEO block mainly promotes solubilization in water [28]. The reduction of $AgNO_3$ by ascorbic acid was conducted at room temperature (ca. 22 °C) in aqueous solutions of PEO-*b*-PMAA and the anionic surfactant sodium dodecyl sulfate (SDS) [17]. Briefly, 9 mL of solution containing PEO-*b*-PMAA (10 mg), SDS (typically, 0.1 mmol), and ascorbic acid (0.2 mmol) was prepared first. Then, 1 mL of 0.2 M $AgNO_3$ was added under vigorous stirring, which gave a final PEO-*b*-PMAA concentration of 1 $g\,L^{-1}$ and final reactant ($AgNO_3$ and ascorbic acid) concentrations of 0.02 M. After 1 min of stirring, the solution was allowed to stand for 24 h, followed by centrifugation and washing with water repeatedly. The collected products were characterized with scanning electron microscopy (SEM), transmission electron microscopy (TEM), X-ray diffraction (XRD), thermogravimetric analysis (TGA), and density measurements.

Received: May 29, 2002
Final version: July 23, 2002

[1] F. Caruso, *Chem. Eur. J.* **2000**, *6*, 413.
[2] Z. Zhong, Y. Yin, B. Gates, Y. Xia, *Adv. Mater.* **2000**, *12*, 206.
[3] A. B. Bourlinos, M. A. Karakassides, D. Petridis, *Chem. Commun.* **2001**, 1518.
[4] C. E. Fowler, D. Khushalani, S. Mann, *J. Mater. Chem.* **2001**, *11*, 1968.
[5] K. H. Rhodes, S. A. Davis, F. Caruso, B. Zhang, S. Mann, *Chem. Mater.* **2000**, *12*, 2832.
[6] R. A. Caruso, A. Susha, F. Caruso, *Chem. Mater.* **2001**, *13*, 400.
[7] F. Caruso, X. Shi, R. A. Caruso, A. Susha, *Adv. Mater.* **2001**, *13*, 740.
[8] D. H. W. Hubert, M. Jung, P. M. Frederik, P. H. H. Bomans, J. Meuldijk, A. L. German, *Adv. Mater.* **2000**, *12*, 1286.
[9] H. T. Schmidt, A. E. Ostafin, *Adv. Mater.* **2002**, *14*, 532.
[10] C. E. Fowler, D. D. Khushalani, S. Mann, *Chem. Commun.* **2001**, 2028.
[11] J. Huang, Y. Xie, B. Li, Y. Liu, Y. Qian, S. Zhang, *Adv. Mater.* **2000**, *12*, 808.
[12] X. Gao, J. Zhang, L. Zhang, *Adv. Mater.* **2002**, *14*, 290.
[13] P. Tartaj, T. Gonzalez-Carreno, C. J. Serna, *Adv. Mater.* **2001**, *13*, 1620.
[14] B. Putlitz, K. Landfester, H. Fischer, M. Antonietti, *Adv. Mater.* **2001**, *13*, 500.
[15] D. Walsh, B. Lebeau, S. Mann, *Adv. Mater.* **1999**, *11*, 324.
[16] T. Liu, Y. Xie, B. Chu, *Langmuir* **2000**, *16*, 9015.
[17] L. Qi, J. Li, J. Ma, *Adv. Mater.* **2002**, *14*, 300.
[18] F. Caruso, M. Spasova, V. Salgueirino-Maceria, L. M. Liz-Marzan, *Adv. Mater.* **2001**, *13*, 1090.
[19] D. I. Gittins, A. S. Susha, B. Schoeler, F. Caruso, *Adv. Mater.* **2002**, *14*, 508.
[20] A. B. R. Mayer, W. Grebner, R. Wannemacher, *J. Phys. Chem. B* **2000**, *104*, 7278.
[21] A. G. Dong, Y. J. Wang, Y. Tang, N. Ren, W. L. Yang, Z. Gao, *Chem. Commun.* **2002**, 350.
[22] Y. Kobayashi, V. Salgueirino-Maceira, L. M. Liz-Marzan, *Chem. Mater.* **2001**, *13*, 1630.
[23] V. G. Pol, D. N. Srivastava, O. Palchik, M. A. Slifkin, A. M. Weiss, A. Gedanken, *Langmuir* **2002**, *18*, 3352.
[24] A recent review: H. Cölfen, *Macromol. Rapid Commun.* **2001**, *22*, 219.
[25] L. Qi, H. Cölfen, M. Antonietti, *Angew. Chem. Int. Ed.* **2000**, *39*, 604.
[26] H. Cölfen, L. Qi, *Chem. Eur. J.* **2001**, *7*, 106.
[27] M. Antonietti, M. Breulmann, C. G. Göltner, H. Cölfen, K. K. Wong, D. Walsh, S. Mann, *Chem. Eur. J.* **1998**, *4*, 2493.
[28] D. Zhang, L. Qi, J. Ma, H. Cheng, *Chem. Mater.* **2001**, *13*, 2753.

Fabrication of Diffractive and Micro-optical Elements Using Microlens Projection Lithography**

By *Ming-Hsien Wu* and *George M. Whitesides**

Arrays of optical microstructures—gratings, beam splitters, lenses, mirrors—are useful in many types of devices such as optical processing systems,[1–3] and microelectromechanical systems (MEMS).[4,5] The quality of these elements depends on their surface profiles and uniformity. Arrays of optical elements have been produced by many methods, including conventional photolithography,[6] laser pattern writing,[7] photography,[8,9] plastic molding,[10] interference lithography,[11] ion-beam lithography,[12,13] X-ray lithography,[14] and conventional gray-scale lithography.[15–17] Although these methods produce uniform elements with controlled surface profiles, they require the use of expensive facilities (e.g., mask aligners or laser optical systems) or templates (e.g. master molds or gray-scale photomasks with sub-micrometer resolution). Some of these techniques (e.g., laser pattern writing and photography) produce microelements with limited resolution (> 1 μm); they cannot, as a result, control the surface relief of the elements at sub-micrometer resolution. Techniques such as interference lithography produce microstructures with sizes, periods, and arrangements limited by the incident wavelengths and angles. All these techniques are relatively expensive and inconvenient.

In this paper, we demonstrate a simple, low-cost method for the fabrication of both diffractive optical elements and arrays of micro-optical elements using microlens arrays for projec-

[*] Prof. G. M. Whitesides, Dr. M.-H. Wu
Department of Chemistry and Chemical Biology, Harvard University
12 Oxford Street, Cambridge, MA 02138 (USA)
E-mail: gwhitesides@gmwgroup.harvard.edu

[**] This work was supported by DARPA and MRSEC. We thank Kateri E. Paul for discussions of the processing of photoresist.

  0935-9648/02/2010-1502 $ 17.50+.50/0

tion photolithography. We used these arrays in such a way that each microlens images a common, illuminated pattern of a transparency mask onto an image plane that coincides with a layer of photoresist (Fig. 1a).[18,19] Microlens projection lithography (μLPL) use a microlens array, combined with different transparency masks, to produce arrays of corresponding micropatterns. We have previously described the use of microlens lithography to fabricate arrays of 2D or 3D microstructures with micrometer or sub-micrometer resolution. This technique provides a simple route for the large-area, parallel fabrication of microstructures. The profiles of the microstructures fabricated by this technique can be modified by adjusting the shapes and gray-level distribution of the patterns on transparency masks. This paper demonstrates that these microstructures, with appropriate profiles or coatings, can act as diffraction elements or imaging arrays. We believe this technique will be useful for the fabrication of optical elements such as microlens arrays, micromirror arrays, beam splitters, and diffraction gratings.

In previous articles, we have used several methods[18–20] to fabricate arrays of microlenses. Here, we used the melting of disks of photoresist (Microposit S1800 photoresist for thickness of resist < 3.5 μm, and Microposit SJR 5000 photoresist for thickness ≥ 3.5 μm, Shipley Inc.) to generate the required lenses. We coated a transparent metallic thin film (12 nm Au on 3 nm Ti) on a glass substrate, and fabricated an array of disks of photoresist on the substrate. The height of the photoresist is about 10–20 % of the diameter of the disks of photoresist. We electroplated the metallic thin film with a layer of 200 nm thick copper using a solution for copper electroplating (Techni Copper U, Technic Inc.) The electroplated copper film formed an aperture stop that blocked the transmission of incident illumination on the areas between lenses, and avoided the fogging of the images produced in the photoresist. The substrate was placed on a hot plate and the photoresist was heated and melted at 180 °C for 15 min. The reflow of melted photoresist formed curved, smooth surface profiles under the influence of the surface tension of the molten polymer. Slow cooling of the substrate (15 °C/min) allowed it to harden while preserving its smooth surface. This method generates arrays of high-quality lenses with sizes between 1 μm and 1 mm, and with either circular or non-circular profile in the plane of the support. Figure 1b illustrates the fabrication process schematically.

The microlens array was covered with a transparent elastomeric spacer with a thickness approximately equal to the focal length of the lenses (Fig. 1a). Since the mask is located at a distance far away from the lens array ($D_{mask} \gg r_{microlens}$), the

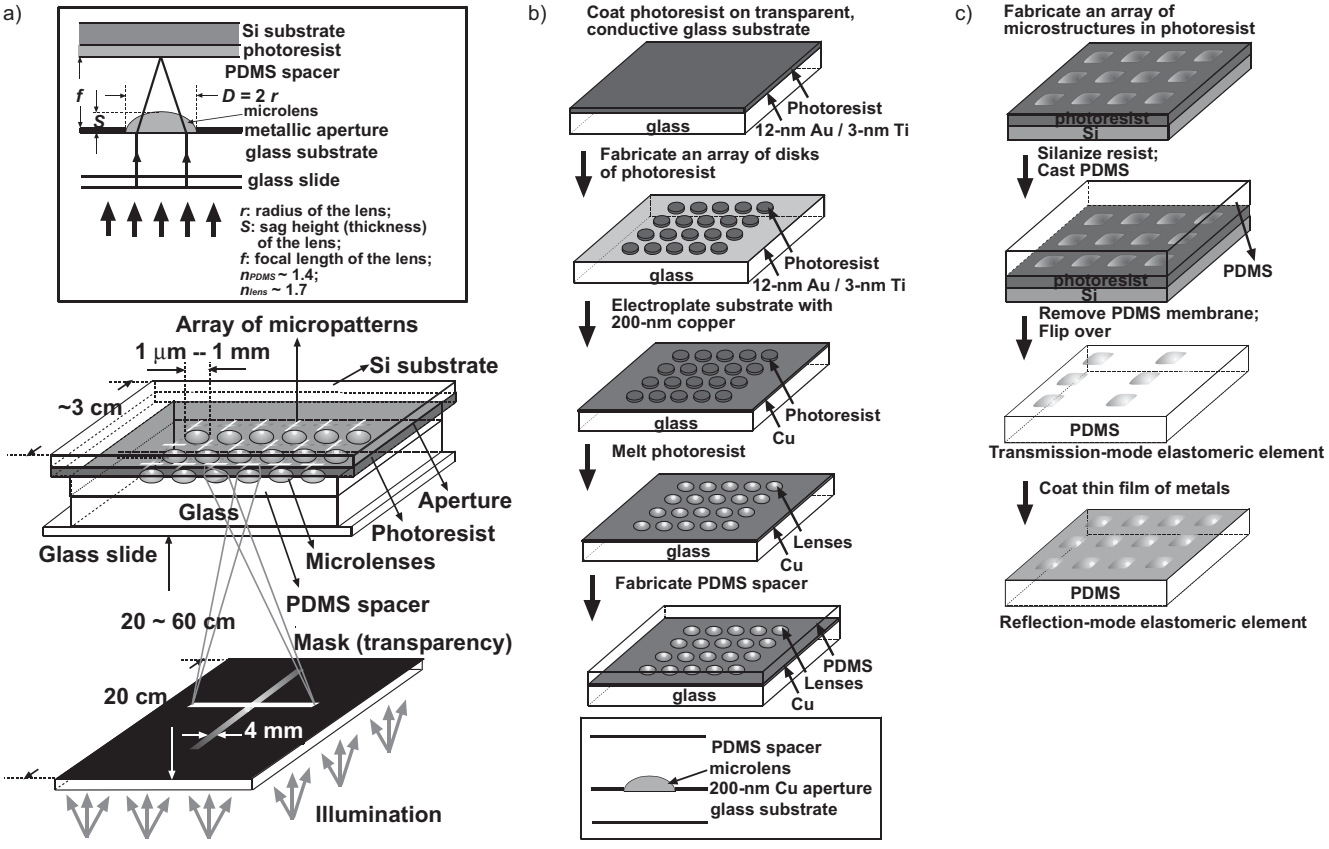

Fig. 1. a) Optical system for microlens projection lithography. The inset shows the concentration of incident illumination by a microlens onto its focal plane. b) Fabrication of microlens arrays using reflow of melted photoresist. Electroplating of a 200 nm thick copper layer formed the aperture stop around the lenses. c) Fabrication of PDMS optical elements using replica molding.

  0935-9648/02/2010-1503 $ 17.50+.50/0

ADVANCED MATERIALS

image distance of the lenses in the array is about the same as their focal length, when imaging occurs through the transparent spacer. To fabricate the spacer, we spin coated a thin film of poly(dimethyl siloxane) (PDMS), Sylgard 184, Dow Corning) onto the lens array. For an array of 10 μm lenses with a numerical aperture ~0.25, the thickness of the PDMS spacer was about 20 μm. A spacer of this thickness was produced by spin coating a mixture of PDMS and heptane (PDMS/heptane = 4.5:1) at 1500 rpm. This elastomeric spacer makes a conformal contact with the photoresist and produces a uniform image distance between the lens array and the photoresist.[18–20]

To perform photolithography, we placed a transparency mask with the designed gray-scale pattern in front of a simple light source (we used either an overhead transparency projector or a UV lamp), and placed a resist-coated silicon substrate in contact with the lens array embedded in its compliant PDMS layer. A diffuser such as a piece of ground glass was placed in front of the light source to produce uniform, incoherent illumination. We used positive photoresist (Microposit S1800 photoresist and Microposit SJR 5000 photoresist, Shipley Inc.) with thicknesses ranging from 1–5 μm. The exposure time was from 10 s to several minutes, depending on the minimum feature size on the mask and the depth of the microstructures. The smaller the feature size, the longer the exposure time; the larger the distance of the mask from the lenses, the longer the exposure time. The profile of the microstructures in the photoresist is a nonlinear function of both the exposure time and the gray-scale distribution of the pattern on the mask.

We used these initial microstructures fabricated in photoresist as masters, and used them to prepare complementary PDMS replicas. These replicas (as 3 mm thick membranes) acted as elastomeric optical elements such as imaging arrays and diffractive elements, depending on their surface profiles. If a thin film of gold (~50 nm thick) was deposited on the surface of the elements, they can function as reflection-mode optical elements such as micromirrors. The fabrication process is illustrated in Figure 1c.

We used μLPL to fabricate five types of optical elements: (i) arrays of refractive microlenses, (ii) arrays of micromirrors, (iii) arrays of diffractive microlenses, (iv) diffraction gratings, and (v) beam splitters. Figure 2a illustrates an array of flower-shaped microlenses on a PDMS membrane fabricated using a gray-scale mask. The mask used for the production of each lens array is shown at the upper left corner of the photomicrograph. The top inset shows the profile of a flower-shaped lens. Figure 1c outlines the procedure used to fabricate these microlenses. We used an array of 10 μm circular lenses with a pitch of 15 μm to fabricate these microlenses. The numerical aperture (N.A.) of the lenses is ~0.25. The middle and bottom insets show the optical micropatterns that a flower-shaped lens produced by focusing the incident illumination at image distances of ~3 μm and 10 μm, respectively.

Figure 2b illustrates an array of binary micromirrors fabricated using the gray-scale mask shown at the corner. We used an array of 40 μm circular lenses with a 50 μm pitch and an

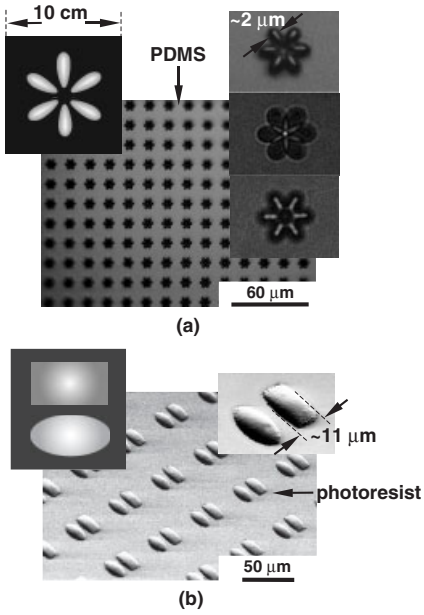

Fig. 2. a) Refractive microlenses fabricated using microlens projection lithography. The photomicrographs show an array of flower-shaped microlenses. b) A square array of rectangular mirrors and ellipsoidal mirrors produced using a square array of 40 μm lenses for microlens projection lithography.

N.A. ~0.125 to fabricate an array of binary microwells. Each 40 μm lens produced a square-shaped microwell and an ellipsoidal microwell. Both microwells have smooth, curved profiles that can act as micromirrors. To fabricate micromirrors, we deposited a thin film of silver (thickness ~50 nm) as a reflective coating onto the microwells.

Figures 3a–c show three arrays of diffractive microlenses with different surface profiles fabricated using three different masks. The masks shown in Figure 3a and 3b have patterns corresponding to 12 zone Fresnel lenses: the first mask has a binary pattern; the second a similar pattern with concentric rings of gradients. We used an array of 100 μm circular lenses to fabricate microlenses for these patterns. The first mask produced an array of binary diffractive lenses, while the second generated an array of blazed diffractive lenses. The depth of the features produced in photoresist is not proportional to the corresponding gray level on the mask due to three factors: (i) the proximity effect, (ii) the aberration of the 100 μm lenses, and (iii) the nonlinearity between the gray level on the mask and the depth of the corresponding features in the developed photoresist. To correct distortions and deviation, we used masks with gray-scale patterns to fabricate these microstructures. We adjusted the gray level of each ring on the mask empirically to optimize the profile of the lenses. The binary mask produced an array of circular phase gratings; the mask with concentric gradients generated an array of circular blazed gratings. Although the surface quality of these gratings did not reach that of standard Fresnel lenses, they acted similar to Fresnel microlenses and performed good-quality imaging. (Their diameters were ca. 65 μm.) We used the micropatterns in photoresist as masters, and cast PDMS onto them to fabricate elastomeric, diffractive microlenses. These diffrac-

  0935-9648/02/2010-1504 $ 17.50+.50/0 *Adv. Mater.* **2002**, *14*, No. 20, October 16

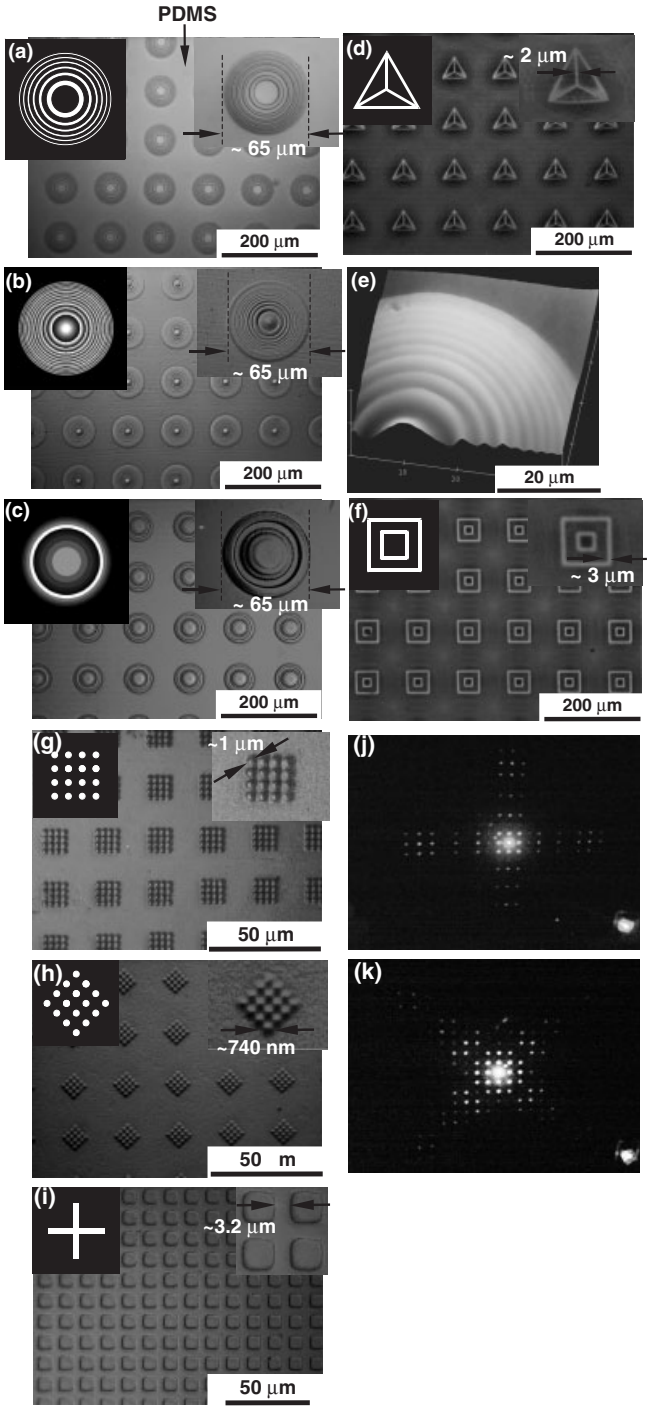

Fig. 3. a–c) Diffractive microlenses fabricated using microlens lithography. These figures show three square arrays of 65 μm diffractive lenses produced using different masks: a) a binary mask with a pattern of a Fresnel lens; b) a mask with a gradient pattern of a Fresnel lens; c) a mask with a pattern of a multi-step diffractive lens; d,f) Arrays of microimages projected by the arrays of diffractive lenses shown in Figures 3a and c, respectively. The transparency masks imaged by the lenses are shown at the corners of the corresponding photomicrographs. e) AFM image of a section of a microlens shown in Figure 3b. g–i) Diffraction elements fabricated using microlens projection lithography. g,h) Two beam splitters that consist of dot arrays with different orientations; j,k) The diffraction patterns produced by the beam splitters shown in Figures 3g and h, respectively. i) A diffraction grating fabricated using a mask with a pattern of a cross.

tive lenses work well as imaging microelements and produce high-quality images. The arrays of optical micropatterns shown in Figure 3d were generated by the arrays of diffractive microlenses (and the masks shown in the insets) as shown in Figure 3a. Figure 3e shows an AFM image of a section of the diffractive lenses shown in Figure 3b. Figure 3c shows an array of multi-step diffractive lenses produced using a multi-gray-level mask. As shown in Figure 3f, these lenses perform good-quality imaging. These figures demonstrate that μLPL can produce multi-step microstructures that function as optical imaging elements. Conventional technologies such as contact photolithography require the use of multiple masks, multiple exposures, and high-precision alignment equipment to fabricate multi-step microstructures. Compared with conventional methods, μLPL is a simple route that can fabricate these microstructures in one exposure.

Figures 3g and 3h shows the surface profiles of two diffractive elements produced using the array of 10 μm circular lenses for gray-scale microlens lithography. These two elements have the same period (15 μm) and the same pattern of microstructures (a 4×4 square array of circular dots). The orientations of the microstructures are different by 45°. Figure 3i shows an optical grating produced using a mask with rectangular lines for μLPL. This figure demonstrates that μLPL may provide a simple route for the fabrication of optical gratings without the use of high-precision optical or mechanical facilities used in conventional methods. Figures 3j and 3k illustrate the diffraction patterns of the corresponding elements shown in Figure 3g and 3h with an incident illumination from a He-Ne laser ($\lambda = 632$ nm). Both elements act as beam splitters. These patterns demonstrate that microlens lithography can modify the surface profiles of diffraction gratings and beam splitters, and thus modulate the distribution of intensity of arrays of spots produced by these elements.

The performance of gray-scale μLPL can be characterized by several factors: (i) diffraction-limited resolution W, (ii) the depth of focus (DOF) Z, and (iii) aberration of the imaging system. The first two factors can in general be expressed by Equations 1 and 2:

$$\delta x = K_1 \times \lambda/\text{N.A.} \quad (1)$$

$$\delta z = K_2 \times \lambda/\text{N.A.}^2 \quad (2)$$

where λ is the incident wavelength and N.A. is the numerical aperture. K_1 and K_2 are parameters that depend on the lithographic process.[21] Lens arrays with higher N.A. can produce microstructures with higher resolution. They can generate smaller pixels in photoresist and produce denser microstructures with higher resolution in their image field. Since DOF is inversely proportional to the square of N.A., the use of high N.A. lens array reduces the depth of high-quality features in photoresist. There is thus a compromise between the resolution and depth of the features produced in photoresist.

  0935-9648/02/2010-1505 $ 17.50+.50/0

ADVANCED MATERIALS

High N.A. also reduces the image fields of the lenses: that is, they produce high-definition images over smaller areas. Features generated on the peripheral area of the image field have lower resolution, due to off-axis aberration such as field curvature. For a given N.A., the aberration of a lens scales with the diameter of the lens.[22] Thus the use of smaller lenses can reduce the influence of the aberration on the quality of the microstructures.

Since we used broadband illumination to expose the photoresist, the chromatic aberration of the lens array could reduce the resolution of the microstructures in photoresist. To minimize this aberration, a narrow-band filter can be placed in front of the light source, or a light source producing narrow-band illumination can be used for exposure. Since we used lenses with diameters less than 100 μm, the short optical paths in the imaging process reduce the dispersion of light focused through the lenses. In our experiments, the chromatic aberration of smaller microlenses (< 30 μm) does not seriously influence the resolution of microstructures. The resolution is primarily influenced by the profile of the lenses.

Microlens lithography with gray-scale masks produces high-quality microlenses, micromirrors, beam splitters, and diffraction gratings over areas at the scale of cm^2. This technique has several characteristics that are useful in the fabrication of repetitive 3D microstructures: (i) It generates arrays of microstructures with controlled profiles using a single step of photolithography, and it does not require the use of chromium masks or mask aligners. (ii) One lens array, when combined with different transparency masks, can produce a variety of microstructures with different profiles. This technique provides a simple route for rapid prototyping of repetitive 3D microstructures. (iii) The use of elastomeric spacers makes it easy to achieve uniform image distances and minimizes the variation of microstructures in photoresist. It protects the lens array from physical damage, and also minimizes the possible damage of photoresist during the contact-mode lithographic process. (iv) Exposures can, in principle, be carried out over a large area. This characteristic minimizes or eliminates the requirement for steppers. (v) The process can be adapted to work (with certain distortion of patterns) on non-planar surfaces.

This technique also has some disadvantages: microstructures produced on the peripheral areas of image fields of a lens array are generated by oblique illumination, and their resolution is reduced due to off-axis aberration of the lenses. The resolution of the microstructures is higher on the central image field, and it gradually degrades toward the peripheral area. It is not uniform over the whole illuminated areas. In addition, this technique produces only repetitive, simple microstructures with the area of each structure less than 1 mm^2. Although this technique eliminates the use of steppers, it cannot generate non-repetitive, complicated microstructures over large areas.

Arrays of microstructures in photoresist produced by this technique can be transferred to other materials using techniques such as etching, electroplating, and molding. We believe this technique will be useful for the fabrication of functional devices that consist of repetitive microstructures.

Received: January 25, 2002
Final version: July 25, 2002

[1] C. Van Berkel, B. P. McGarvey, J. A. Clarke, *Pure Appl. Opt.* **1994**, *3*, 177.
[2] C. Berger, N. Collings, R. Vökel, M. T. Gale, T. Hessler, *Pure Appl. Opt.* **1997**, *6*, 683.
[3] R. H. Anderson, *Appl. Opt.* **1979**, *18*, 477.
[4] A. Tuantranont, V. M. Bright, J. Zhang, W. Zhang, J. A. Neff, Y. C. Lee, *Sens. Actuators A* **2001**, 91, 363.
[5] E. S. Kolesar, P. B. Allen, J. W. Wilken, J. T. Howard, *Thin Solid Films* **1998**, *332*, 1.
[6] J.-B. Yoon, J.-D. Lee, C.-H. Han, E. Yoon, C.-K. Kim, *Proc. SPIE–Int. Soc. Opt. Eng.* **1998**, *3512*, 358.
[7] C. P. Christensen, *Proc. SPIE–Int. Soc. Opt. Eng.* **1994**, *2045*, 141.
[8] E. Navarrete-Garcia, S. Calixto, *Appl. Opt.* **1998**, *37*, 739.
[9] S. Calixto, G. P. Padilla, *Appl. Opt.* **1996**, *35*, 6126.
[10] Y. Xia, E. Kim, X.-M. Zhao, J. A. Rogers, M. Prentiss, G. M. Whitesides, *Science* **1996**, *273*, 347.
[11] K. M. Baker, *Appl. Opt.* **1999**, *38*, 352.
[12] S. T. Davies, D. A. Hayton, K. Tsuchiya, *Proc. SPIE–Int. Soc. Opt. Eng.* **1996**, *2880*, 248.
[13] Y. Fu, N. K. A. Bryan, *Rev. Sci. Instrum.* **2000**, *71*, 2263.
[14] V. A. Kudryashov, L. Sing, *Microelectron. Eng.* **2001**, *57–58*, 819.
[15] W. Däschner, P. Long, R. Stein, C. Wu, S. H. Lee, *J. Vac. Sci. Technol. B* **1996**, *14*, 3730.
[16] P. Long, W. Däschner, E. Johnson, S. H. Lee, *Proc. SPIE–Int. Soc. Opt. Eng.* **1997**, *3010*, 105.
[17] C. Gimkiewicz, D. Hagedorn, J. Jahns, E.-B. Kley, F. Thomas, *Appl. Opt.* **1999**, *38*, 2986.
[18] M.-H. Wu, G. M. Whitesides, *Appl. Phys. Lett.* **2001**, *78*, 2273.
[19] M.-H. Wu, G. M. Whitesides, *Appl. Opt.* **2002**, *41*, 2575.
[20] M.-H. Wu, K. E. Paul, J. Yang, G. M. Whitesides, *Appl. Phys. Lett.* **2002**, *80*, 3500.
[21] S. Wittekoek, *Microelectron. Eng.* **1994**, *23*, 43.
[22] N. Bareket, *J. Opt. Soc. Am.* **1979**, *69*, 1311.

Mechanically Stable Zeolite Monoliths with Three-Dimensional Ordered Macropores by the Transformation of Mesoporous Silica Spheres**

By *Angang Dong*, *Yajun Wang*, *Yi Tang*,* *Yahong Zhang*, *Nan Ren*, and *Zi Gao*

Three-dimensional ordered macroporous (pore size > 100 nm) materials have recently aroused great interest in materials science research, owing to their unusual properties and wide potential applications, ranging from photonic crystals to advanced catalysts and adsorbents.[1] Currently, a typical procedure for their fabrication involves three steps, namely: the production of a three-dimensional template from monodisperse latex particles (e.g., silica and polymer beads), the infiltration and solidification of the desired precursors (e.g., metal alkoxides and nanoparticles) inside the template, and the removal of

[*] Prof. Y. Tang, A. Dong, Y. Wang, Y. Zhang, N. Ren, Prof. Z. Gao
Laboratory of Molecular Catalysis and Innovative Materials
Department of Chemistry, Fudan University
Shanghai 200 433 (China)
E-mail: ytang@fudan.ac.cn

[**] This work was supported by the Major State Basic Research Development Program (Grant No. 2 000 077 500), the NSFC (Grant No. 29 873 011), the Foundation for University Key Teacher by the Ministry of Education and the Doctoral fund of Education Ministry.

  0935-9648/02/2010-1506 $ 17.50+.50/0